Structural health monitoring data fusion for in-situ life prognosis of composite structures

Eleftheroglou, Nick; Zarouchas, Dimitrios; Loutas, Theodoros; Alderliesten, Rene; Benedictus, Rinze

DOI
10.1016/j.ress.2018.04.031

Publication date
2018

Document Version
Final published version

Published in
Reliability Engineering and System Safety

Citation (APA)
Eleftheroglou, N., Zarouchas, D., Loutas, T., Alderliesten, R., & Benedictus, R. (2018). Structural health monitoring data fusion for in-situ life prognosis of composite structures. *Reliability Engineering and System Safety*, *178*, 40-54. https://doi.org/10.1016/j.ress.2018.04.031

Reliability Engineering and System Safety 178 (2018) 40–54

Contents lists available at ScienceDirect

Reliability Engineering and System Safety

journal homepage: www.elsevier.com/locate/ress

Structural health monitoring data fusion for in-situ life prognosis of composite structures

Nick Eleftheroglou[a,*], Dimitrios Zarouchas[a], Theodoros Loutas[b], Rene Alderliesten[a], Rinze Benedictus[a]

[a] Structural Integrity & Composites Group, Aerospace Engineering Faculty, Delft University of Technology, 2629 HS Delft, The Netherlands
[b] Applied Mechanics Laboratory, Department of Mechanical Engineering & Aeronautics, University of Patras, Rio 26500, Greece

ARTICLE INFO

Keywords:
Data fusion
Remaining useful life
Prognostic performance metrics
Structural health monitoring
Composite structures

ABSTRACT

A novel framework to fuse structural health monitoring (SHM) data from different in-situ monitoring techniques is proposed aiming to develop a hyper-feature towards more effective prognostics. A state-of-the-art Non-Homogenous Hidden Semi Markov Model (NHHSMM) is utilized to model the damage accumulation of composite structures, subjected to fatigue loading, and estimate the remaining useful life (RUL) using conventional as well as fused SHM data. Acoustic Emission (AE) and Digital Image Correlation (DIC) are the selected in-situ SHM techniques. The proposed methodology is applied to open hole carbon/epoxy specimens under fatigue loading. RUL estimations utilizing features extracted from each SHM technique and after data fusion are compared, via established and newly proposed prognostic performance metrics.

1. Introduction

When the degradation process of a component/structure is monitored, maintenance can be planned dynamically (condition based maintenance) instead of periodically (scheduled maintenance) based on health monitoring data [1,2]. This requires prognostic capability for predicting the damage evolution of the degradation state of the component/structure in the future. The word prognostics is originally a Greek word which means to know in advance, to foresee [3]. In engineering, prognostics are defined as the estimations of the remaining useful life (RUL) of a component, which is degrading during its operation time [4].

In general, prognostic modeling options can be classified into four types; reliability based, physics-based, data-driven and hybrid [3,5]. In industrial applications of components and machinery almost all the aforementioned approaches have found applications. In structural prognostics on the other hand, relevant literature is quite limited. Chiachio et al. [6,7] and Corbetta et al. [8] have recently utilized a Bayesian filtering framework that incorporates information from empirical damage models and health monitoring data in order to enable predictions of the remaining useful life of composite materials. They utilized state-of-the-art empirical models for matrix cracking, delaminations and crack growth to predict through the use of particle filtering the future damage states and thus estimate the remaining life. However, the parameters of those empirical models, i.e. the fitting parameters of Paris relation power-law relationship [9,10], depend on the type of failure, loading case, geometry and stacking sequence, limiting the applicability of these models to coupons rather than in complex composite structures.

In contrast, the main idea behind prognostic data-driven models is to use health monitoring representative training data from the studied component (independent on its complexity in terms of loading conditions, geometry etc.), in order to estimate a mathematical model's parameters ($\boldsymbol{\theta}$). Then, based on the trained model a probability density function of the RUL can be determined. Characteristic examples of data-driven prognostic approaches for composite materials/structures are presented hereafter.

Liu et al. [11] utilized Gaussian processes, as a mathematical model, to perform non-linear regression. Gaussian process was trained with acoustic emission (AE) data and Lamb wave signals in order to estimate the RUL of composite beams. By comparing the RUL estimations of Lamb wave signals and AE data, it can be seen that Lamb's RUL estimations were better than AE's RUL estimations. The same research team in [12] proposed a prognostic methodology, which consisted of real time sensor signals from strain gages, direct cross-correlation analysis and a Gaussian process trained with off-line data to perform the non-linear regression prognostic task. Notched carbon/epoxy composite specimens under fatigue loading were used. Eleftheroglou and Loutas

* Corresponding author.
E-mail addresses: n.eleftheroglou@tudelft.nl (N. Eleftheroglou), d.zarouchas@tudelft.nl (D. Zarouchas), loutas@mech.upatras.gr (T. Loutas), r.c.alderliesten@tudelft.nl (R. Alderliesten), r.benedictus@tudelft.nl (R. Benedictus).

https://doi.org/10.1016/j.ress.2018.04.031
Received 7 June 2017; Received in revised form 16 April 2018; Accepted 29 April 2018
Available online 26 May 2018
0951-8320/

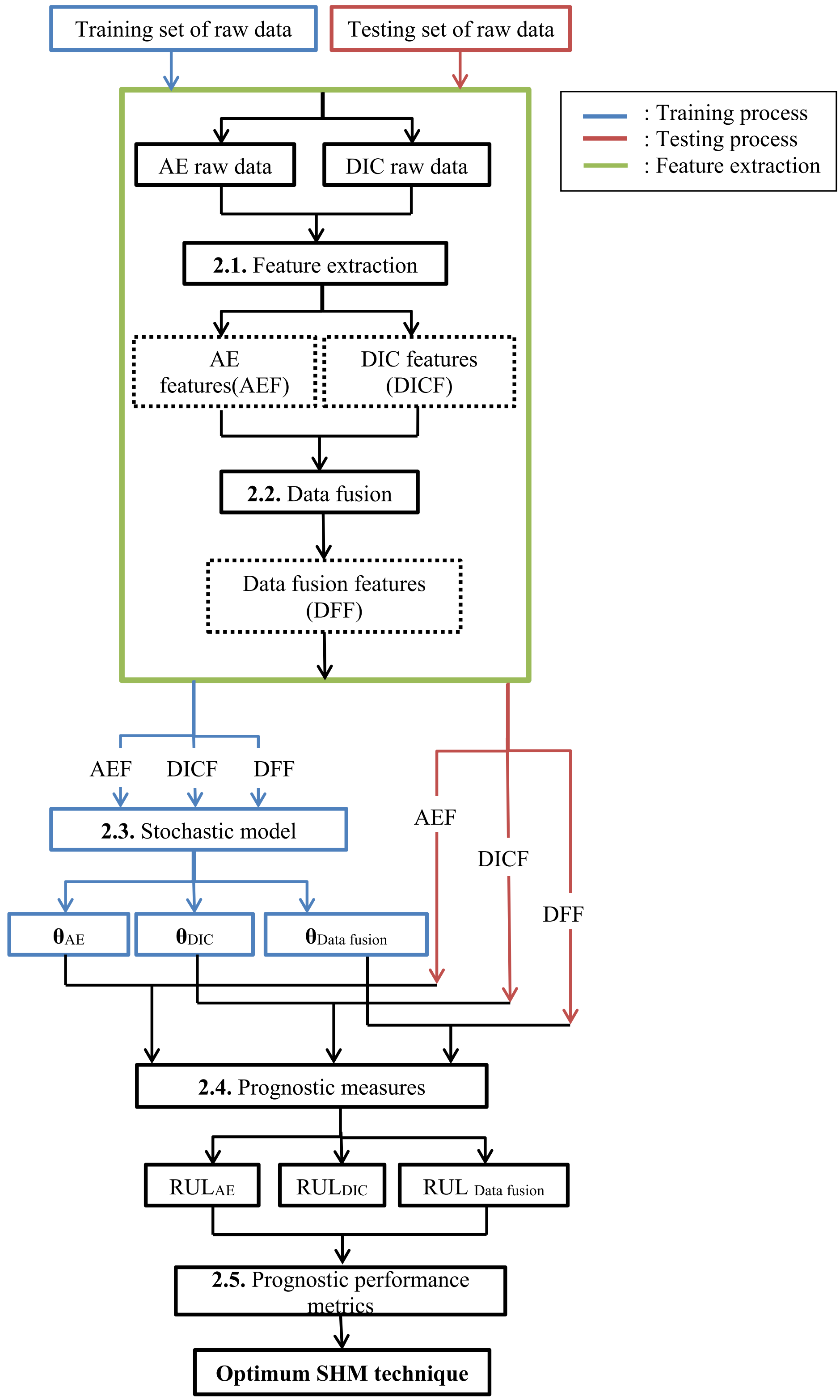

Fig. 1. Proposed RUL prediction methodology.

[13] and Eleftheroglou et al. [14] proposed the use of a multi-state degradation model, i.e. the Non-Homogenous Hidden Semi Markov Model (NHHSMM), for the in-situ prognostics of open hole carbon/epoxy specimens under fatigue loading. They used AE [13] or strain measurements [14] to estimate the parameters of the NHHSMM and successfully used it to obtain RUL estimates in unseen data with uncertainty quantification. In Loutas et al. [15] two data-driven prognostic models, i.e. NHHSMM and Bayesian Neural Networks (BNN), utilizing AE measurements, were compared via several prognostic performance metrics. Fatigue tests were performed in open hole carbon/epoxy specimens. The NHHSMM clearly exceled the performance metrics at this study. The aforementioned case studies represent some prognostic models that are encountered in the literature on application to composite structures/materials.

In the SHM community [16,17], it has been long known that various health monitoring techniques have different sensitivities to composite structures' failure mechanisms. The process of extracting information from different monitoring techniques and integrate them into a consistent, accurate and reliable data set is known as data fusion and it has been already successfully applied to damage diagnostics [18–20]. In principle, data fusion can be implemented in three levels; raw multi-sensor data fusion, feature-level fusion and decision-level fusion. Raw data fusion should be treated with caution as sensor recordings may have different acquisition, pre-filtering and amplification settings. In addition, raw data fusion needs to have as input commensurate data. As a result, feature-level and decision-level fusion are more common [21].

By combining features extracted from different sensors or monitoring techniques and integrating them into a single feature, is known to enhance the diagnostics performance [21,22]. Data fusion for structural prognostics purposes has never been attempted according to the authors best knowledge. We expect the prognostic performance to be improved when fusing SHM data from various monitoring techniques. In order to quantify this statement various prognostic performance metrics are employed for the comparison.

In this study a data-driven approach is followed utilizing a sophisticated stochastic model, i.e. the Non-Homogeneous Hidden Semi Markov model (NHHSMM), since the physics of composite structures' damage evolution is not yet fully understood or explained by a mathematical model of global validity and recent advances in SHM technologies enable us to continuously monitor composite structures during their operation time [23]. Furthermore, we follow the feature-level data fusion strategy combining features extracted from two different SHM techniques and introducing new hyper-features of higher monotonicity that it is expected to improve the RUL estimations. Acoustic Emission (AE) and Digital Image Correlation (DIC) techniques are employed to monitor the damage evolution during fatigue loading. The first provide data related to the failure mechanisms that occur after energy release due to damage formulation in micro-scale level and the latter measures surface strain fields.

The main objective of this paper is to investigate the potential of SHM data fusion for structural prognostics of composite structures. Emphasis is given in improving the prognostic performance. The main contributions of the present study are listed below:

- A novel data fusion methodology is proposed that is able to combine heterogeneous monitoring data i.e. AE and DIC data.
- Application of a sophisticated data-driven prognostic model, i.e. NHHSMM, for the very first time with fused data.
- Two new prognostic performance metrics are proposed i.e. Modified Mann–Kendal (MMK) monotonicity metric and Confidence Intervals Distance Convergence (CIDC) metric.

The remainder of this paper is organized as follows. In Section 2, the selected RUL prediction methodology is described where its feature extraction process, SHM data fusion methodology, prognostic model and prognostic performance metrics are discussed. A case study analysis follows in Section 3 and finally the paper is concluded in Section 4.

2. Remaining useful life prediction methodology

The goal of the remaining useful life prediction methodology is to estimate the composite structure's RUL probability density function. In order to facilitate that, health monitoring data are utilized to train a mathematical model (i.e. estimate its parameters $\boldsymbol{\theta}$), which will provide the RUL estimations. Fig. 1 summarizes the RUL prediction methodology, which is proposed in this paper.

In the framework of this study, SHM data i.e. AE and DIC data during constant amplitude fatigue tests in open-hole composite coupons are used. The available SHM data can be divided to training and testing sets. However, the raw AE and DIC data include noise so a feature extraction process is required in order to produce features with strong prognostic suitability. A detailed description of the term 'prognostic suitability' is given in Section 2.1. In the case that more than one monitoring techniques are available, a data fusion strategy can be implemented to enhance the prognostic performance of the available SHM data (Section 2.2). The current study proposes a new feature-level data fusion strategy, which combines features from the AE and DIC techniques.

Based on the available training SHM features the parameters $\boldsymbol{\theta}$ of the mathematical model, that is utilized to provide with the RUL predictions, are estimated (Section 2.3). In the present study we utilize a stochastic multi-state degradation model, such as NHHSMM, based on its successful implementation in our previous investigations [13,14]. Three different NHHSMMs are trained after using features extracted from the training set of AE, DIC and fused AE & DIC. After training the respective NHHSMMs, health monitoring observations from an unseen case (testing set) may feed the models after the relevant pre-processing and obtain the mean/median RUL estimations and the associated 90% confidence intervals (Section 2.4). Special metrics are introduced (Section 2.5) so as to evaluate the performance of the SHM data.

2.1. Data pre-processing and feature extraction

A set of metrics in order to illustrate a feature extraction process has been proposed in the relevant literature and consists of monotonicity, prognosability and trendability [24–27]. Monotonicity characterizes a parameter's general increasing or decreasing trend, prognosability measures the spread of a parameter's failure value and finally, trendability indicates whether degradation histories of a specific parameter have the same underlying trend.

In order to produce features with strong prognostic capability, the aforementioned metrics can be used as feature design properties. In this paper, the feature extraction process is based on monotonicity since a feature that is sensitive to the degradation process is desirable to have a monotonic trend [25,26,28]. Prognosability is excluded from the present feature extraction process since NHHSMM dictates that the last observation of the monitoring data must be unique and common for all the degradation histories [13,29,30]. The feature extraction process does not take into account the influence of trendability since the target of this work is to identify monotonicity's influence in prognostics.

A second key element of the NHHSMM is that the monitoring data's domain should be discrete [13,29,30]. Different methods, such as vector quantization and clustering can be used to discretize the available monitoring data [31]. In this paper the unsupervised k-means algorithm is used to cluster and quantize the features extracted from the SHM data. The target of using k-means algorithm is to find the optimal number of discrete levels, which delivers features with maximum monotonicity. To quantify the monotonicity we introduce the Modified Mann–Kendall (MMK) criterion, Eq. (1).

$$\mathrm{MMK} = \frac{\sum_{\mathrm{i}=1}^{\mathrm{D}} \sum_{\mathrm{j}=1,\mathrm{j}>\mathrm{i}}^{\mathrm{D}} (t_j - t_i)\cdot \mathrm{sgn}(\mathrm{y}(t_j) - \mathrm{y}(t_i))}{\sum_{\mathrm{i}=1}^{\mathrm{D}} \sum_{\mathrm{j}=1,\mathrm{j}>\mathrm{i}}^{\mathrm{D}} (t_j - t_i)} \cdot 100\% \tag{1}$$

where $\mathrm{y}(t_i)$ the feature value at time of measurement t_i, D the number of measurements and $sgn(x) = \begin{Bmatrix} -1 \; if \; x < 0 \\ 0 \; if \; x = 0 \\ 1 \; if \; x > 0 \end{Bmatrix}$.

The advantages of the MMK criterion, over the classical Mann–Kendal criterion [32], are explained below:

- Mann–Kendal (MK) values have not any informative meaning. For example, in the current case study the MK values' range is (10^5, 4×10^5). However, MMK value as defined in (1) expresses a percentage of monotonicity in the range $[-1,1]$. If MMK = 1 the degradation history is strictly increasing, if MMK = -1 the degradation history is strictly decreasing. In any other case the degradation history is not strictly monotonic.

- Secondly, based on the MMK criterion each degradation history has the same monotonicity weight. On the other hand, the classical MK criterion is biased since a longer degradation history gives a higher MK value.

The objective of the feature extraction process as implemented in this study, is to obtain quantized degradation histories with the as high monotonicity as possible using features from AE data, DIC data and fused ones.

2.2. Data fusion methodology

The fusion scheme receives as inputs the quantized AE and DIC features, where the following equation explains the rationale behind the fusion process.

$$f_t(DIC, AE) = \sum_{j=0}^{M} \sum_{i=0}^{i+j\leq M} a_{ij} \cdot DIC^{j} \cdot AE^{i} \tag{2}$$

where f_t is the fused output feature, a_{ij} are constant coefficients that control the weight of the exponential DIC and AE features' product and M the maximum polynomial degree power that these features can use. The Modified Mann–Kendal (MMK) criterion, Eq. (1), is adopted to enable the data fusion process and is expressed in Eq. (3). MMK is used as an objective function to be maximized and thus determine which polynomial degree M and constant coefficients a_{ij} give the most monotonic fused feature.

$$\mathrm{MMK}(a_{ij}, M) = \frac{\left[\sum_{k=1}^{K}\sum_{i=1}^{d_k}\sum_{j=1,j>i}^{d_k}\left(t_j^{(k)} - t_i^{(k)}\right)\cdot \mathrm{sgn}\left(f_j^{(k)}(a, M) - f_i^{(k)}(a, M)\right)\right]}{\left[\sum_{k=1}^{K}\sum_{i=1}^{d_k}\sum_{j=1,j>i}^{d_k}\left(t_j^{(k)} - t_i^{(k)}\right)\right]}\cdot 100\% \tag{3}$$

where K is the number of available training degradation histories (e.g. the number of tested specimens), $f_i^{(k)}$ the fused feature value at time of measurement $t_i^{(k)}$ for the kth specimen, d_k the number of the kth specimen's measurements and

$$sgn(x) = \begin{Bmatrix} -1 \ if \ x<0 \\ 0 \ if \ x=0 \\ 1 \ if \ x>0 \end{Bmatrix}$$

The constant polynomial coefficients a_{ij}, for each polynomial degree M, are based on the optimization problem described in Eq. (4) with the monotonicity obtained by the MMK criterion as the objective function. For the aforementioned optimization problem, different optimization techniques were used i.e. Nelder–Mead, Neural Networks, Particle Swarm Optimization (PSO), Genetic Algorithms and OptQuest/NLP (OQNLP). For this exercise, it was found that OQNLP [33] is the most efficient optimization technique regarding the computational time of the parameters a_{ij} and M. The unconstrained optimization problem is formulated as:

$$\alpha_{ij}^{*} = \underset{a_{ij}}{\mathrm{argmax}}\,(\mathrm{MMK}(a_{ij}, M)) \tag{4}$$

In conclusion, the outputs of the proposed data fusion methodology are the optimum polynomial degree M and the optimum constant coefficients a_{ij} based on the MMK monotonicity, Eq. (4).

2.3. Stochastic modeling

The aim of the NHHSMM is to correlate the damage accumulation process, which is normally hidden, with the SHM data (observations). NHHSMM has the capabilities, as a state space model, to achieve this correlation as it consists of a bi-dimensional stochastic process where the first process forms a finite Semi Markov chain (SMC) not directly observed i.e. the damage sequence and the second process, conditioned on the first, forms a sequence of conditionally independent random variables i.e. the SHM features. Only a brief description of the model is presented hereafter in order to aid the coherence of the paper's structure. The interested reader can refer to Moghadass and Zuo [29,30], who set the original framework, as well as Eleftheroglou and Loutas [13], who implemented it in structural prognostics, for a more detailed description.

The model's parameters $\boldsymbol{\theta}$ are obtained via a maximum likelihood estimation approach. Moghadass and Zuo [29,30] proposed a method for defining the Maximum Likelihood Estimator (MLE) $\boldsymbol{\theta}^*$ of the model parameter $\boldsymbol{\theta}$, which maximizes the likelihood function $L(\boldsymbol{\theta},\boldsymbol{y}^{(1:K)})$,

$$L(\theta, \boldsymbol{y}^{(1:K)}) = \prod_{k=1}^{K} \Pr(\boldsymbol{y}^{(k)}|\theta) \xRightarrow{L'=\log(L)} L'(\theta, \boldsymbol{y}^{(1:K)}) = \sum_{k=1}^{K} \log(\Pr(\boldsymbol{y}^{(k)}|\theta))$$

$$\theta^{*} = \underset{\theta}{\mathrm{argmax}}\left(\sum_{k=1}^{K} log(Pr(\boldsymbol{y}^{(k)}|\theta))\right) \tag{5}$$

where $\mathbf{y}^{(k)}$ is the kth degradation history, K is the total number of available degradation histories. Setting initial values for $\boldsymbol{\theta}$ and solving the aforementioned optimization problem the model's parameters are estimated from the training dataset (fused or standalone).

2.4. Prognostic measures

Conditional on the testing SHM dataset and model's parameters $\boldsymbol{\theta}$, prognostic measures can be calculated via the conditional reliability function [29,30]. The conditional reliability function, $R\left(t\middle|y_{1:t_p}, L>t_p, \theta\right) = Pr\left(L>t\middle|y_{1:t_p}, L>t_p, \theta\right)$, represents the probability that the composite structure continues to operate after a time t, less than the life-time L ($L>t$), further than the present time t_p given that the composite structure has not failed yet ($L>t_p$), conditional on the testing SHM dataset $y_{1:tp}$ up to t_p and the model's parameters $\boldsymbol{\theta}$. In this study the mean, median and confidence intervals of RUL constitute the prognostic measures. They can be calculated via the cumulative distribution function (CDF) of RUL. The CDF of RUL is defined at any time point via the conditional reliability according to the following Eq. (6):

$$Pr\left(RUL_{t_p}\leq t|y_{1:t_p}, \theta\right) = 1 - R\left(t + t_p\middle|y_{1:t_p}, \theta\right) \tag{6}$$

2.5. Prognostic performance metrics

Eight prognostic performance metrics are employed in order to evaluate the predictive performance of the three NHHSMMs trained with the different types of SHM features. Six of them are metrics widely used in literature [34,35] i.e. Precision, Mean Squared Error (MSE), Mean Absolute Percentage Error (MAPE), Median Absolute Percentage Error (MdAPE), Cumulative Relative Accuracy (CRA), Convergence (C_{Em}). The aforementioned prognostic performance metrics are defined in the following:

1. Precision

Precision $=\sqrt{\frac{\sum_{i=1}^{D}(E_m(t_i) - \overline{E_m}(t_i))^2}{D-1}}$, where $\overline{E_m}$ is the mean value of error E_m and

$E_m(t_i) = RUL_{actual}(t_i)$-$meanRUL(t_i)$ and t_i ε [1,D] is the discrete time moment when the ith SHM observation is recorded.

2. Mean Squared Error (MSE)

$$\text{MSE} = \sqrt{\frac{\sum_{i=1}^{D} (E_m(t_i))^2}{D}}.$$

3. Mean Absolute Percentage Error (MAPE)

$$\text{MAPE} = \frac{1}{D}\sum_{i=1}^{D}\left|\frac{100\cdot E_m(t_i)}{\text{RUL}_{\text{actual}}(t_i)}\right|$$

4. Median Absolute Percentage Error (MdAPE)

, where $\text{Emd}(\text{ti}) = \text{RUL}_{\text{actual}}(\text{t}_i) - \text{medianRUL}(\text{t}_i)$.

5. Cumulative Relative Accuracy (CRA)

$$\text{CRA} = \frac{\sum_{i=1}^{D} \text{RA}(t_i)}{D} \text{ where } \text{RA}(t_i) = 1 - \left|\frac{E_m(t_i)}{RUL_{actual}(t_i)}\right|.$$

6. Convergence (C_{Em})

$$C_{Em} = \sqrt{(x_c - t_1)^2 + y_c^2}$$
where

$$x_c = \frac{\sum_{i=1}^{D-1} (t_{i+1}^2 - t_i^2)\cdot|E_m(\text{i})|}{2\cdot\sum_{i=1}^{D-1} (t_{i+1} - t_i)\cdot|E_m(\text{i})|} \text{ and } y_c = \frac{\sum_{i=1}^{D-1} (t_{i+1} - t_i)\cdot E_m(\text{i})^2}{2\cdot\sum_{i=1}^{D-1} (t_{i+1} - t_i)\cdot|E_m(\text{i})|}.$$

7. Monotonicity

The prognostic's function monotonicity can be measured based on the proposed Modified Mann–Kendal (MMK) monotonicity criterion where $y(t_i)$ is replaced with $meanRUL(t_i)$. In case of the studied function, which is the RUL prediction function, the preferable value of MMK $= -1$ since it is expecting that the composite structure's RUL is decreasing monotonically during its lifetime.

8. Confidence Intervals Distance Convergence (CIDC)

Goebel et al. [36] stated that as the amount of data increases during the fatigue life, the confidence intervals distance should converge. In order to quantify this statement, a new metric is introduced; the Confidence Intervals Distance Convergence (CIDC). This metric is an extension of the metric of convergence in [34] but in this case the centroid is under the confidence intervals distance curve. In general, lower Euclidian distance means faster convergence. Let (x_c, y_c) be the center of mass of the area under the confidence intervals distance curve, then the CIDC can be represented by the Euclidean distance between the (x_c, y_c) and the origin (t_1,0), where:

$$\text{CIDC} = \sqrt{(x_c - t_1)^2 + y_c^2}$$

where

$$x_c = \frac{\sum_{i=1}^{D-1} (t_{i+1}^2 - t_i^2)\cdot(UCI(\text{i}) - \text{LCI(i)})}{2\cdot\sum_{i=1}^{D-1} (t_{i+1} - t_i)\cdot(UCI(\text{i}) - \text{LCI(i)})},$$
$$y_c = \frac{\sum_{i=1}^{D-1} (t_{i+1} - t_i)\cdot(UCI(\text{i}) - \text{LCI(i)})^2}{2\cdot\sum_{i=1}^{D-1} (t_{i+1} - t_i)\cdot(UCI(\text{i}) - \text{LCI(i)})}$$

and

UCI, LCI the upper and lower selected confidence intervals.

Fig. 2 demonstrates how the CIDC metric works in two hypothetical sets of confidence intervals 1 and 2. The confidence intervals in case 2 converge faster than confidence intervals 1, see Fig. 2(a). In Fig. 2(b) the Euclidean distance of the mass center 2 and the origin ($\text{CIDC}_2 = 9.7419$) is lower than the Euclidian distance of the mass center 1 and the origin ($\text{CIDC}_1 = 10.5048$) thus, the CIDC metric is validated.

3. Case study

Seven open-hole carbon/epoxy specimens, with [0/ ± 45/90]2 s, lay-up were manufactured via the autoclave process with the following details: dimensions [300 mm x 30 mm] and a central hole of 6 mm diameter. These specimens were subjected to fatigue loading with maximum amplitude 90% of the static tensile strength ($F_{\text{ult}} = 42.66$ kN), $R = 0$ and $f = 10$ Hz. The tests were executed in a MTS 100 kN universal test machine and they run up to failure. A stereovision system was used to perform 3D full field DIC measurements in order to measure strain distribution on the specimen surface during the entire fatigue test. In addition, an AE system was used in order to perform AE measurements. Fig. 3 presents the experimental set-up, the fatigue loading and the data acquisition process. The reader can refer to Eleftheroglou et al. [37] for a more detailed description of the experimental campaign. Table 1 presents the cycles to failure for the tested specimens.

3.1. Digital image correlation feature extraction

DIC technique enabled strain measurements in the entire surface of the specimen. Fig. 4 presents the axial strain distribution, strain in the load direction, as calculated at the maximum loading during the fatigue test of specimen02.

Based on the analytical model of Lekhnitskii [38], which calculates the effect of a notch on the stress/strain distribution, the green rhomboid point (half a diameter distance for the hole center in the transverse direction), highlighted at the picture of 0 cycles, was chosen as the critical point to extract the axial strains. Fig. 5 presents the seven axial strain degradation histories, which were extracted for the aforementioned critical point.

As discussed earlier, the final SHM feature should be presented in a discrete form by the clusters V, that can be calculated using the Modified Mann–Kendal criterion. The MMK converges for the number of clusters V equals to 25 for the DIC data, as Fig. 6 presents. Fig. 7 presents the final clustered axial strain data after the thresholding process.

3.2. Acoustic emission feature extraction

1/A (1/amplitude) was found to have the highest monotonic observation sequences and it was selected as the AE feature to use. Similar to DIC measurement, 1/A was calculated cumulatively in periodic time windows of 500 cycles. The respective degradation histories for seven specimens are shown in Fig. 8.

Although the MMK monotonicity converges for number of clusters ≥ 18, see Fig. 9, $V = 25$ was selected for the AE data equal to the number of clusters for strain data. This way, the data fusion process becomes more efficient as the normalization of the AE and DIC features is avoided. Fig. 10 presents the final clustered AE data.

3.3. SHM data fusion results

The results of the optimization study, Eq. (4), are presented for various polynomial degrees M in Fig. 11. The MMK monotonicity converges for a polynomial degree $M \geq 5$. Therefore, the polynomial degree is selected as $M = 5$.

For determined polynomial degree $M = 5$, Table 2 summarizes the optimization results regarding the constant coefficients a_{ij}.

The fused features for polynomial degree $M = 5$ and the aforementioned polynomial coefficients a_{ij} are depicted in Fig. 12.

Fig. 13 presents the MMK monotonicity for each SHM feature i.e. AE, DIC and fused data and it is observed that the fused data has the highest monotonic rate. The data fusion process is presented in Appendix too.

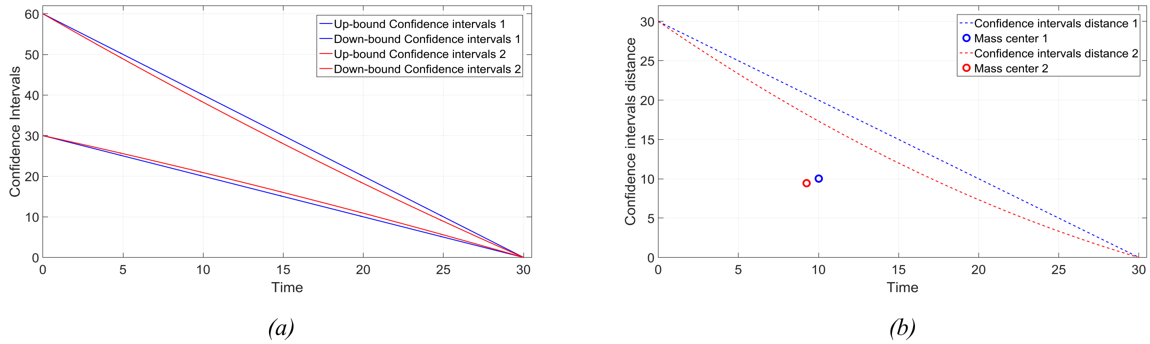

Fig. 2. Validation of Confidence Intervals Distance Convergence metric (a) Hypothetical sets of confidence intervals (b) Mass centers under the confidence intervals distance curves.

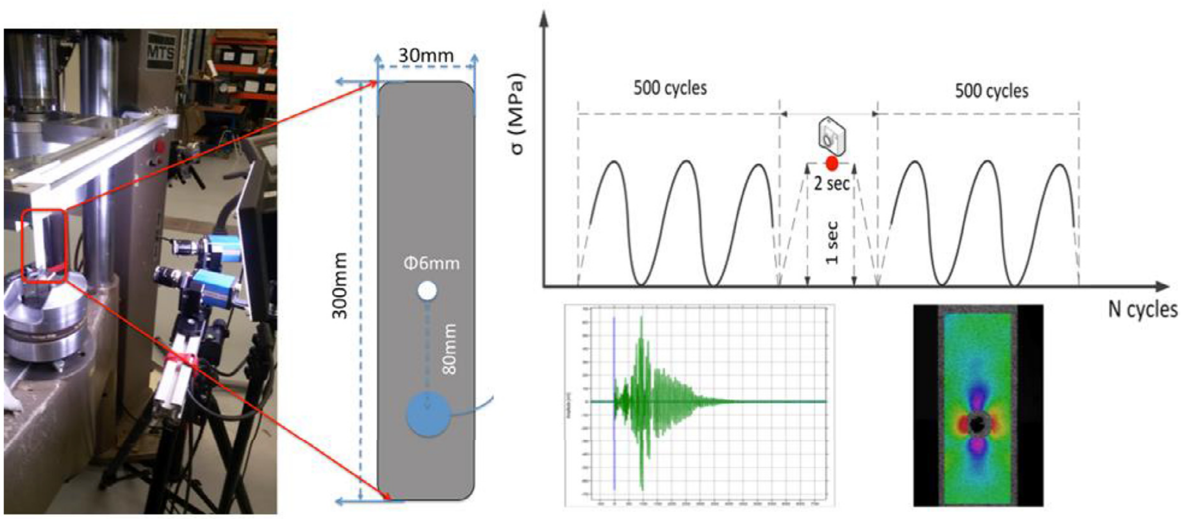

Fig. 3. The experimental set-up and the acquisition data process [37].

Table 1
Cycles to failure of tested coupons.

Specimen #	Fatigue test conditions	Cycles to failure (x 10^3)
A1	$R = 0$	63
A2		25
A3	$f = 10$ Hz	22
A4	$A = 42.66 \times 90\%$ kN	24.5
A5		14
A6	$[0/\pm 45/90]_{2s}$	25
A7		30

3.4. Remaining useful life estimations

Seven degradation histories $\mathbf{Y} = [\mathbf{y}^{(1)},\mathbf{y}^{(2)},\ldots,\mathbf{y}^{(7)}]$ were available for each SHM technique (AE, DIC and fused data). The training dataset employs six degradation histories in order to estimate the NHHSMM's parameters $\boldsymbol{\theta}$ and keeps the seventh degradation history as the testing prognostic dataset.

The mean/median RUL and the 90% confidence intervals can be calculated using Eq. (2). The level of confidence intervals depends on the application, i.e. for aerospace applications 90% and 95% are common values [39] and 90% will be adopted for this study. Figs. 14 and 15 present the RUL estimations of the three available SHM techniques for specimen03 and specimen04, respectively. The choice of presenting the results of those specimens was random, similar results were obtained for the other specimens.

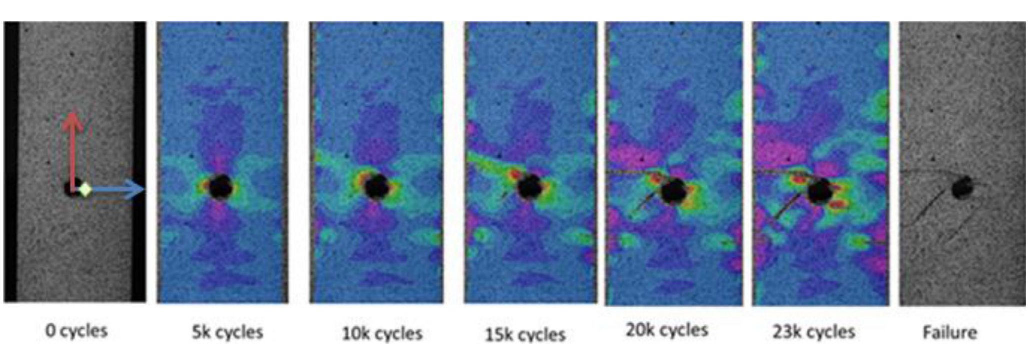

Fig. 4. Axial strain distribution of specimen02.

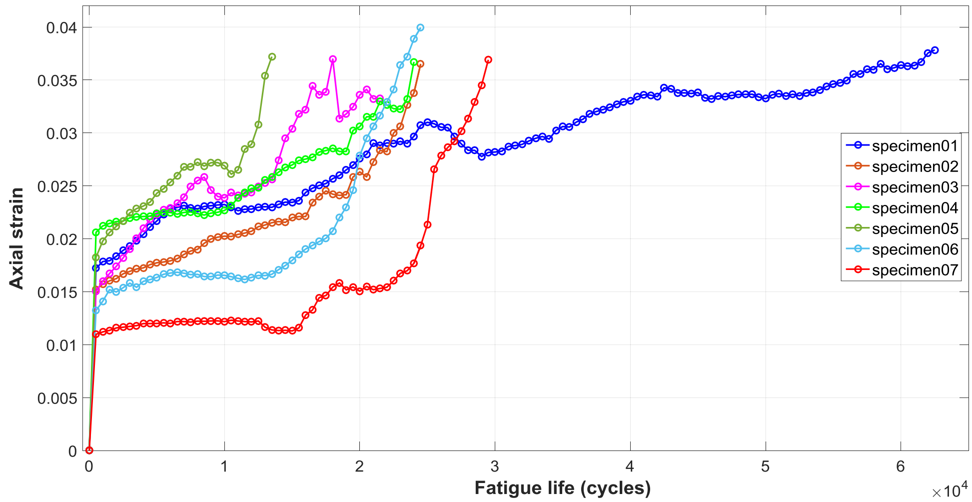

Fig. 5. Axial strain degradation histories of seven open-hole specimens.

The RUL estimations converge quite satisfactorily with the actual RUL values. Based on Figs. 14 and 15 the strain data provides the best RUL estimations, fused data is ranked second while AE provides the worst estimations. In order to quantify these observations we utilize eight prognostic performance metrics.

3.5. Prognostic performance metrics implementation

In Figs. 16–23 the results of the performance metrics, defined in Section 2.5, are presented. Based on these results, it is confirmed that DIC data provides the best RUL estimations since DIC RUL estimations score better in all prognostic performance metrics. For example, based on Fig. 16, AE RUL estimations of specimen01 (SP1) excel at precision metric since the precision of the AE RUL estimations are lower than the precision of the DIC and Fusion RUL estimations. The optimum values of the prognostic performance metrics are following:

Precision: minimum value	CRA: maximum value
MSE: minimum value	Monotonicity: minimum value
MAPE: minimum value	C_{Em}: minimum value
MdAPE: minimum value	CIDC: minimum value

4. Conclusions

A RUL prediction methodology that utilized two different sources of SHM data for remaining fatigue life prognosis in composite structures and a new data fusion methodology, on a feature-level, were presented in this paper. Open-hole carbon/epoxy specimens were subjected to constant amplitude fatigue loading up to failure and DIC and AE techniques were employed, to monitor the fatigue tests and provide the required SHM data. In addition, six prognostic performance metrics were employed and two new were introduced, in order to compare the performance of the RUL estimations. The following conclusions can be withdrawn:

- A new data fusion approach was developed and the main objective was to produce hyper-features with high monotonicity. Although the degradation histories of the fused data had monotonicity higher than the monotonicity of the degradation histories of DIC and AE features, the fused data didn't provide always better estimations, indicating that the requirement of monotonicity is not enough and extra criteria should be involved. Nevertheless, the results demonstrate the potential of the proposed data fusion methodology and its evolvement by adding extra criteria, such as trendability, will enhance the performance of the fused data.
- In order to accommodate the phenomenon of the structural degradation over time and the belief that as the amount of data

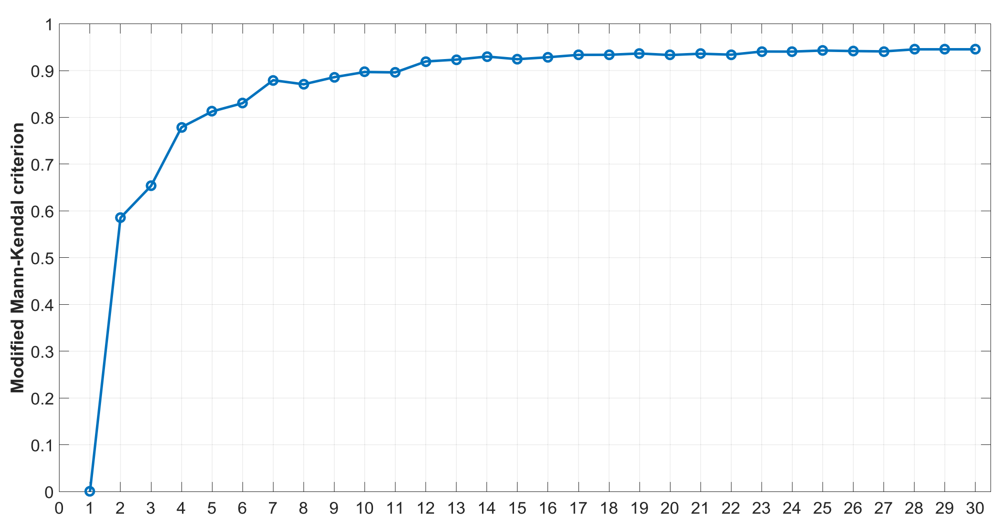

Fig. 6. MMK monotonicity convergence of DIC data versus the number of clusters (V).

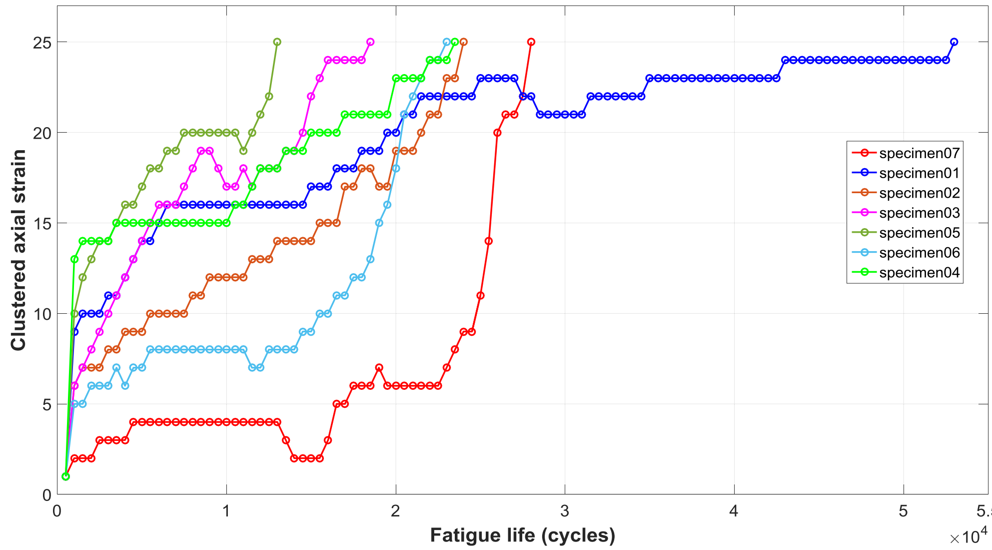

Fig. 7. Clustered axial strain degradation histories of seven open-hole specimens.

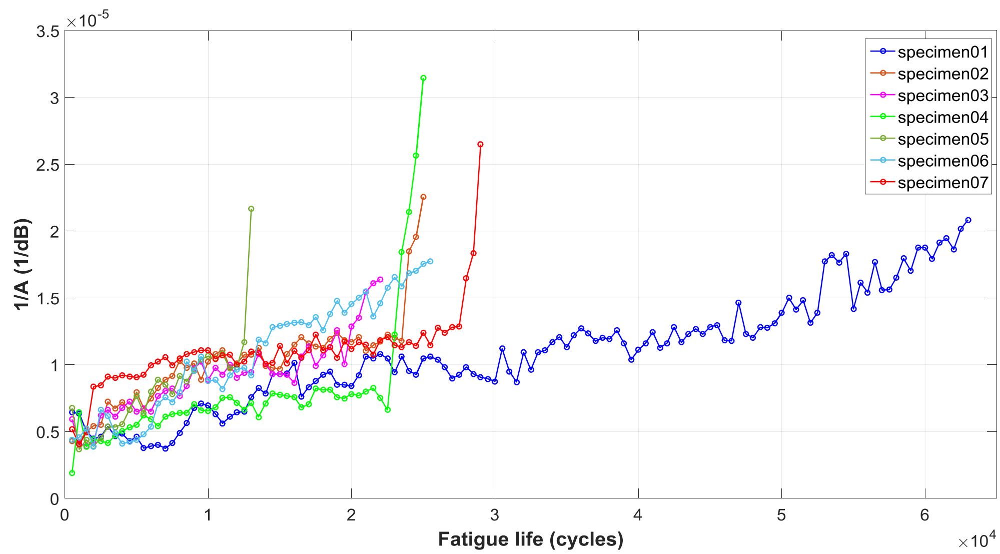

Fig. 8. AE degradation histories of seven open-hole specimens.

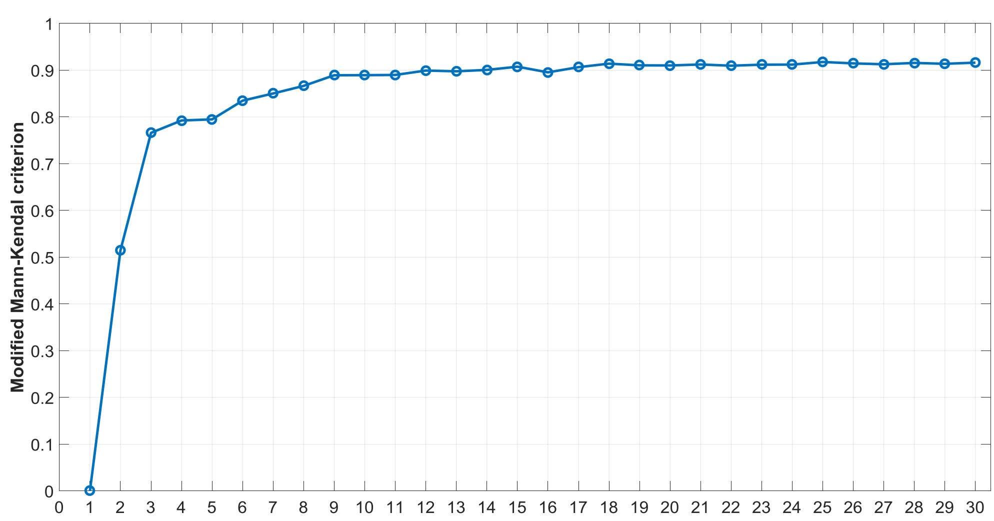

Fig. 9. MMK monotonicity convergence of AE data versus the number of clusters (V).

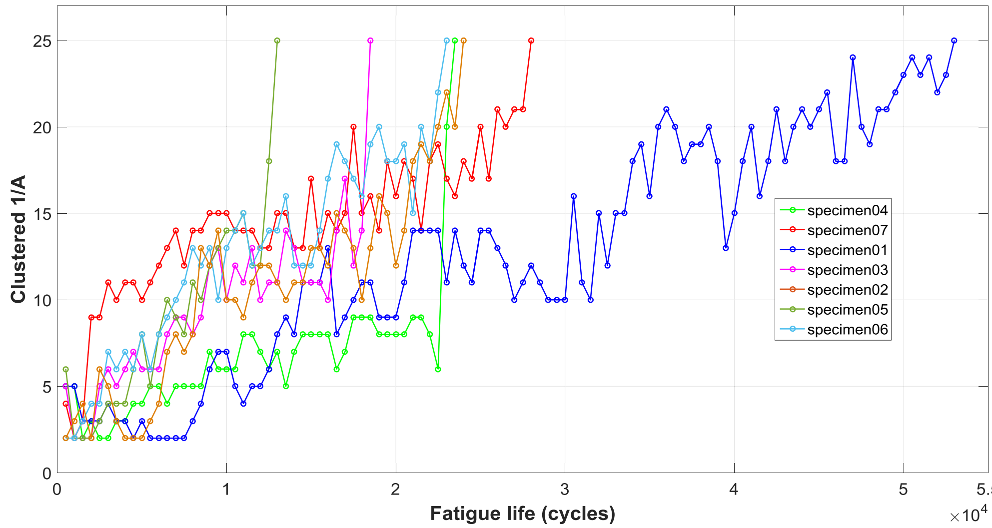

Fig. 10. Clustered AE degradation histories of seven open-hole specimens.

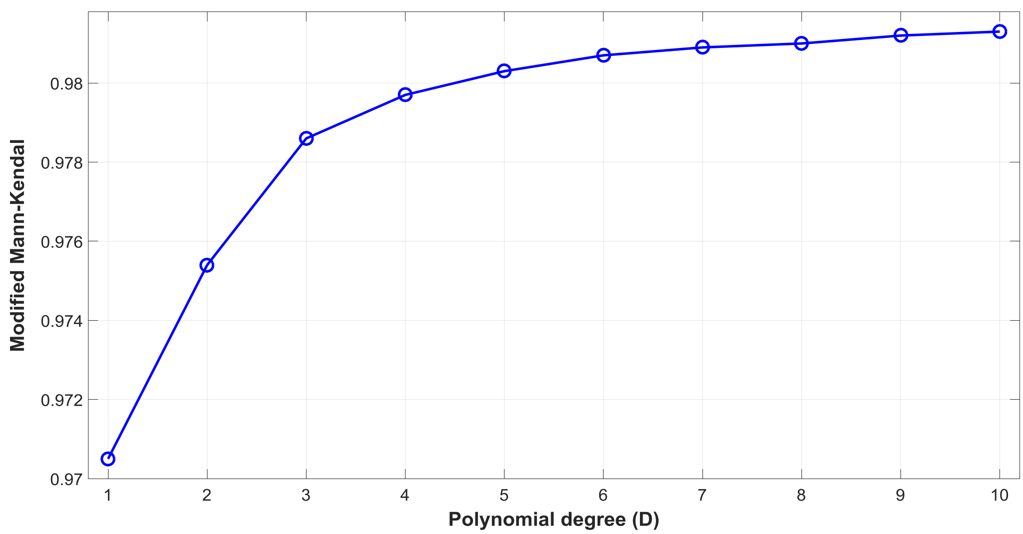

Fig. 11. Modified Mann–Kendal value versus the polynomial degree.

Table 2
Optimization results for $M = 5$.

	AE^0	AE^1	AE^2	AE^3	AE^4	AE^5
DIC^0	−39,955	−953,757	−743,892	471,0798	882,5275	1,985,843
DIC^1	−783,606	1,989,894	−746,044	381,3022	−344,348	0
DIC^2	412,001	411,5522	271,9862	829,036	0	0
DIC^3	−922,063	−183,044	−16,7071	0	0	0
DIC^4	292,6789	906,5035	0	0	0	0
DIC^5	336,2406	0	0	0	0	0

increases the confidence intervals should converge, two new prognostic performance metrics, Modified Mann–Kendal (MMK) monotonicity and Confidence Intervals Distance Convergence (CIDC) were proposed and materialized these statements. Their results were similar to the results of the other metrics and their applicability was verified.

- The feature extraction process for the strain data was straightforward, as after the determination of the critical specimen's point, the axial strain data was extracted via the DIC technique. The well-established analytical model of Lekhnitskii enhanced the feature performance indicating that mechanics can play an informative role on the feature selection process. In contrast, extensive signal processing was performed in order to identify monotonic histories that describe sufficiently the damage accumulation process using AE data.

Consequently, the current work characterizes the DIC data as the optimum prognostic performance data, compare it with the AE and fusion data. This statement is consistent with the selected stochastic model i.e. NHHSMM, the selected data fusion process and the selected prognostic performance metrics.

Considering the importance of delivering a RUL prediction methodology that is generic enough and able to provide reliable estimations, future work includes a new fusion approach that will take into consideration not only the monotonicity but also the trendability of degradation histories, more representative operating conditions, i.e. variable amplitude fatigue, generic element geometries and additional SHM techniques.

Funding

This research did not receive any specific grant from funding agencies in the public, commercial, or not-for-profit sectors.

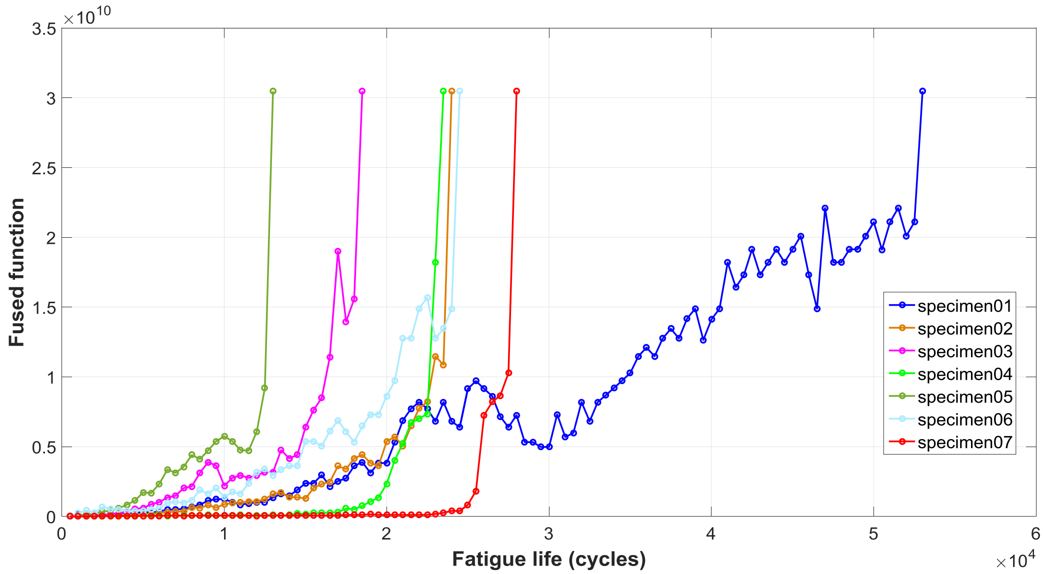

Fig. 12. Fused degradation histories of seven open-hole specimens.

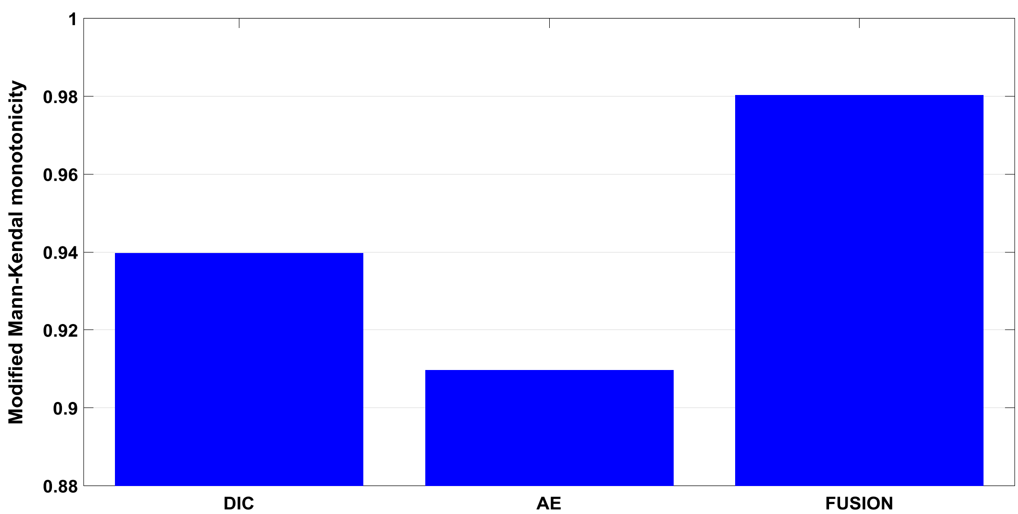

Fig. 13. Comparison between DIC, AE and Fusion MMK monotonicity.

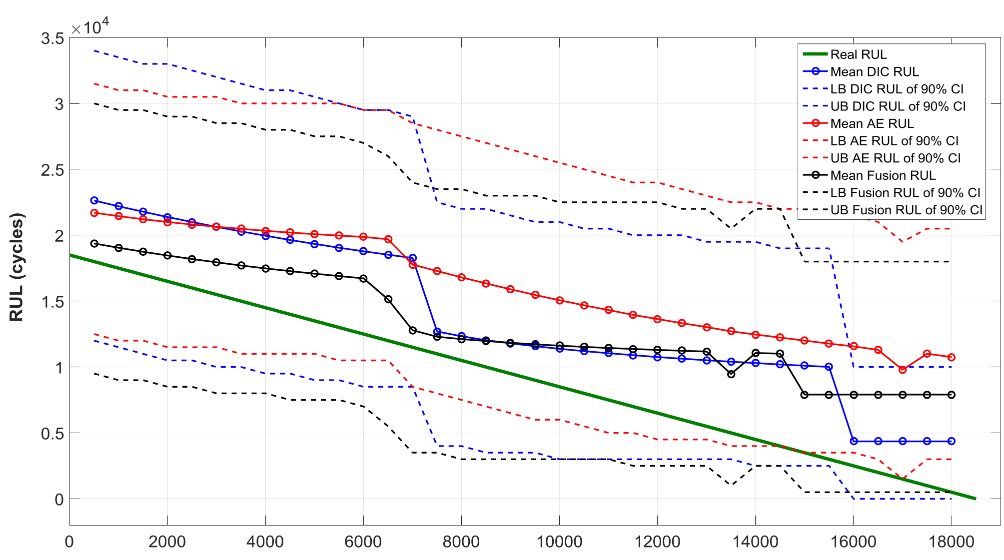

Fig. 14. Estimated mean RUL and 90% confidence intervals for specimen03.

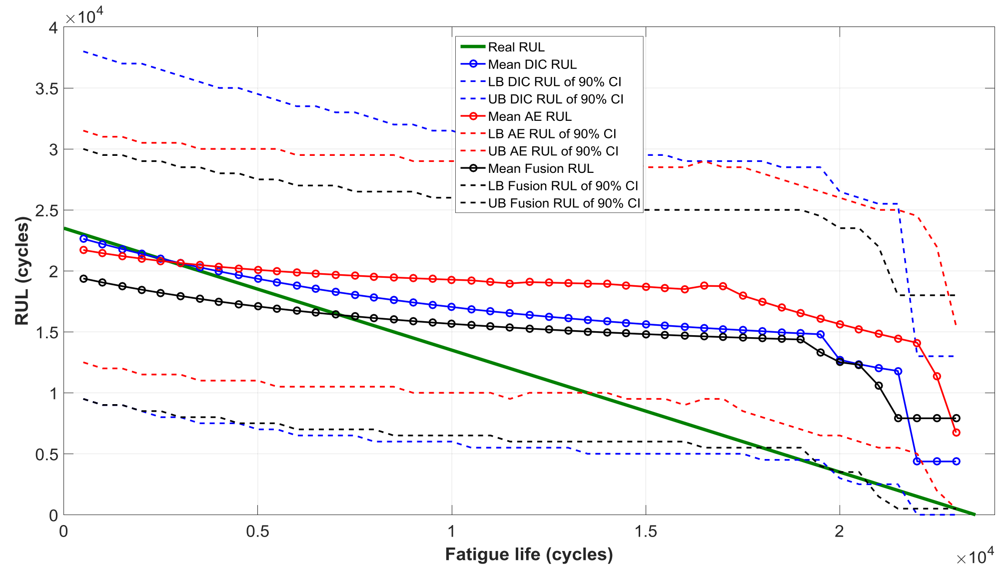

Fig. 15. Estimated mean RUL with 90% confidence intervals for specimen04.

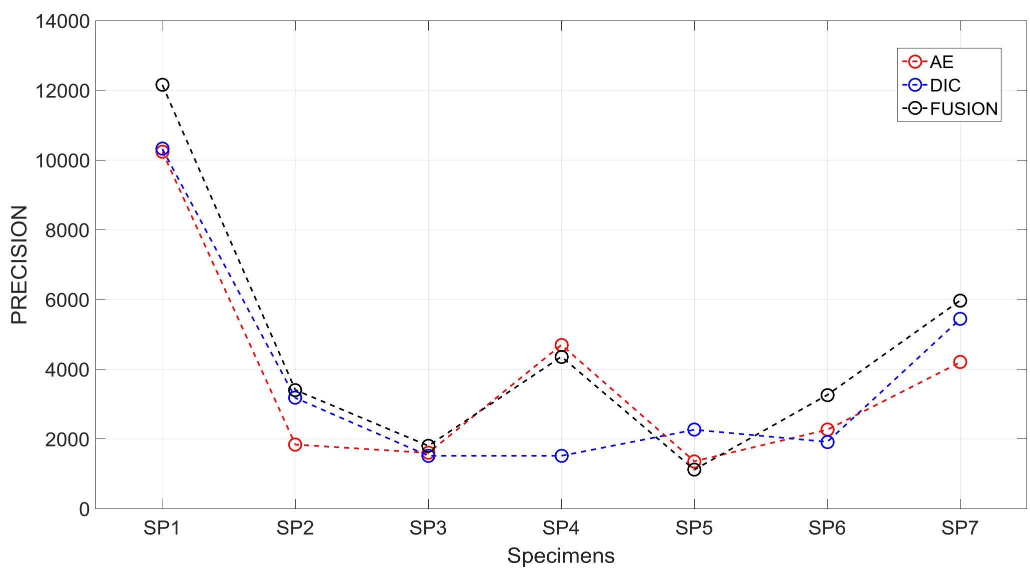

Fig. 16. Precision prognostic performance metric of each specimen and SHM technique.

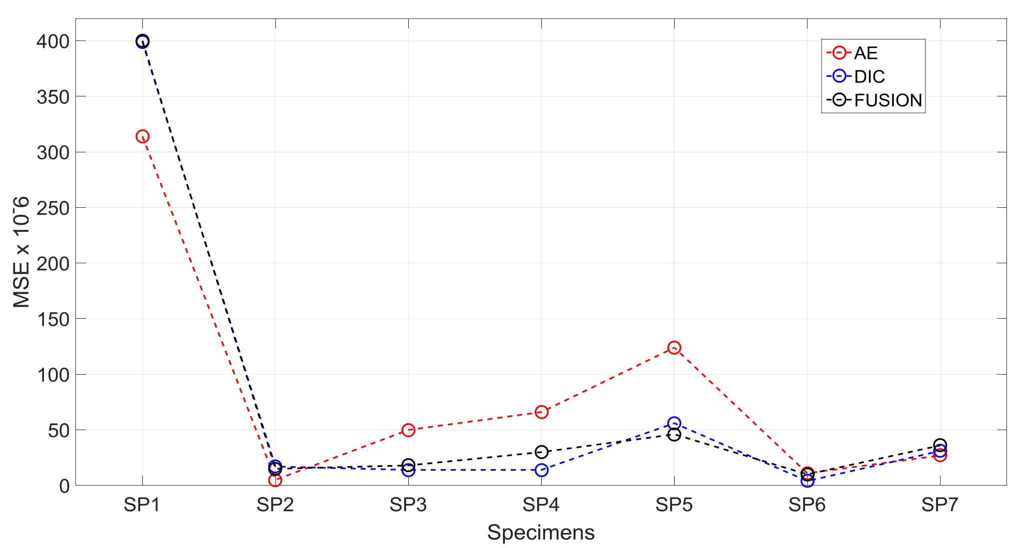

Fig. 17. MSE prognostic performance metric of each specimen and SHM technique.

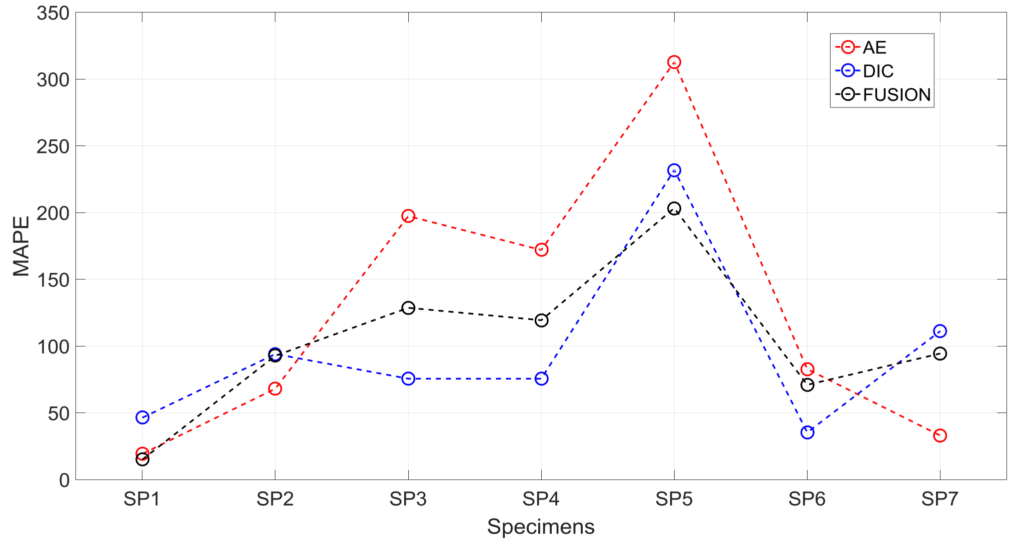

Fig. 18. MAPE prognostic performance metric of each specimen and SHM technique.

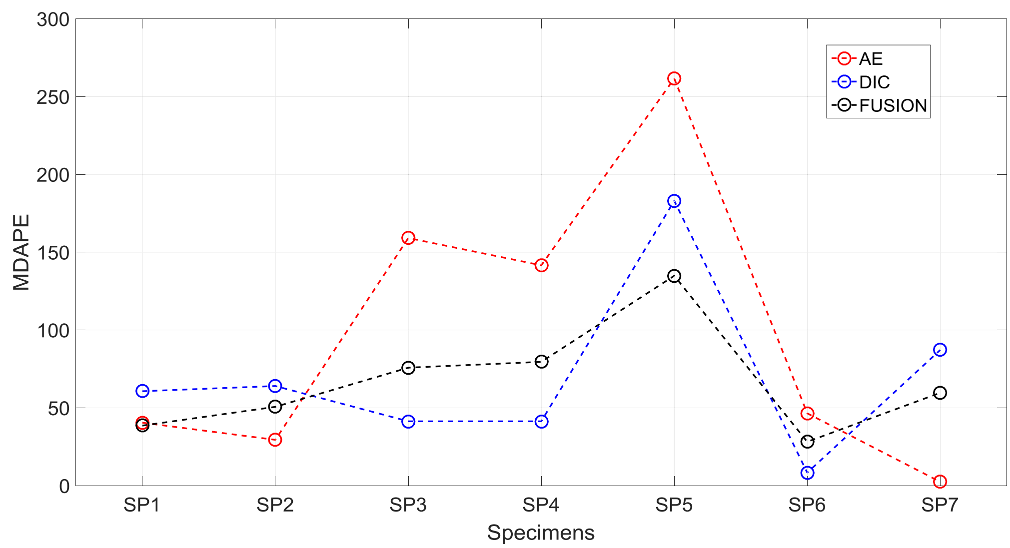

Fig. 19. MDAPE prognostic performance metric of each specimen and SHM technique.

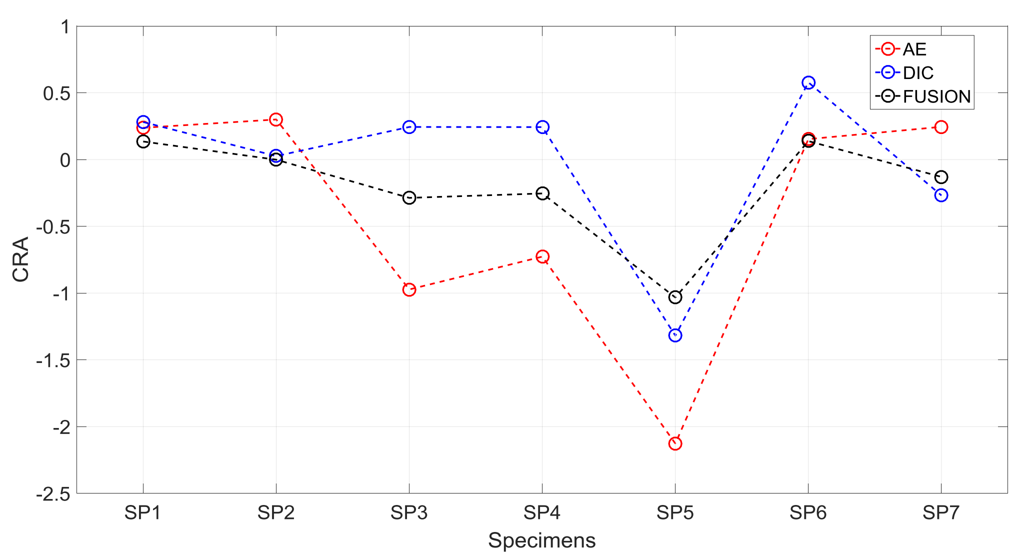

Fig. 20. CRA prognostic performance metric of each specimen and SHM technique.

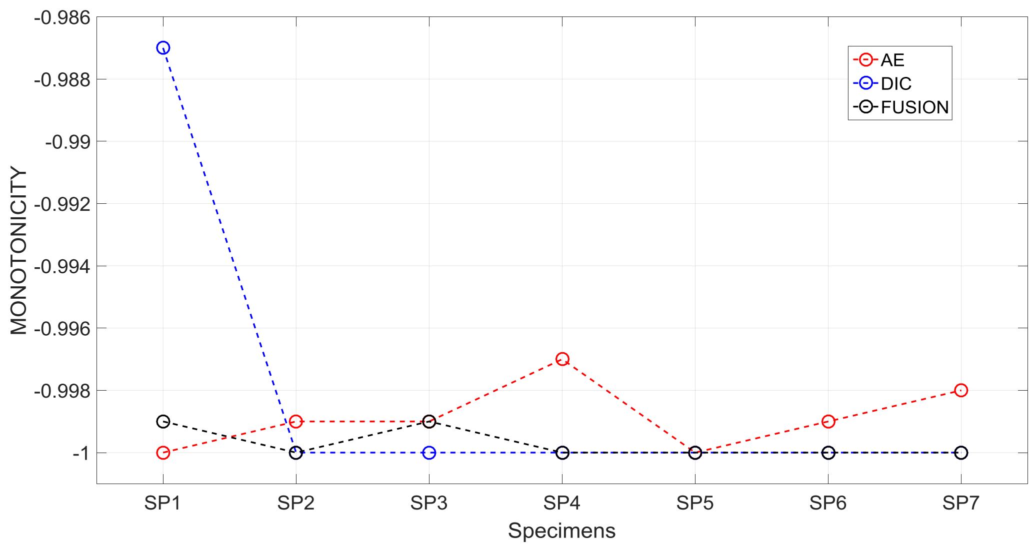

Fig. 21. Monotonicity prognostic performance metric of each specimen and SHM technique.

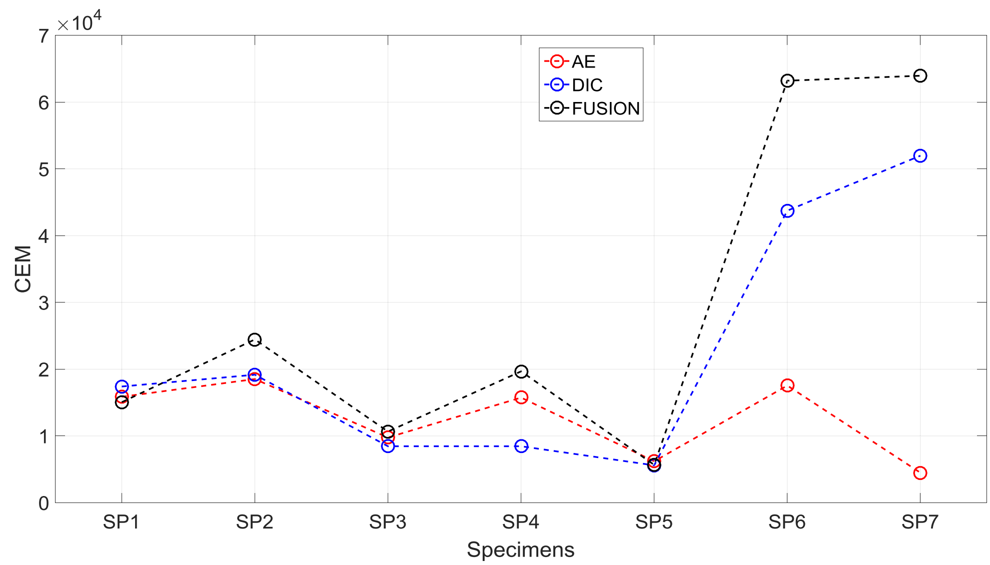

Fig. 22. C_{EM} prognostic performance metric of each specimen and SHM technique.

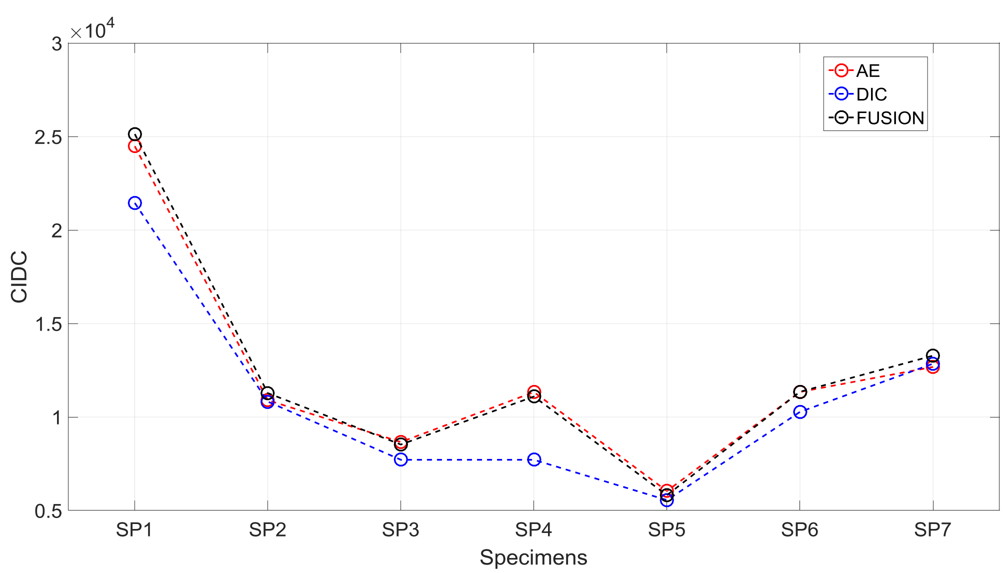

Fig. 23. CIDC prognostic performance metric of each specimen and SHM technique.

Appendix

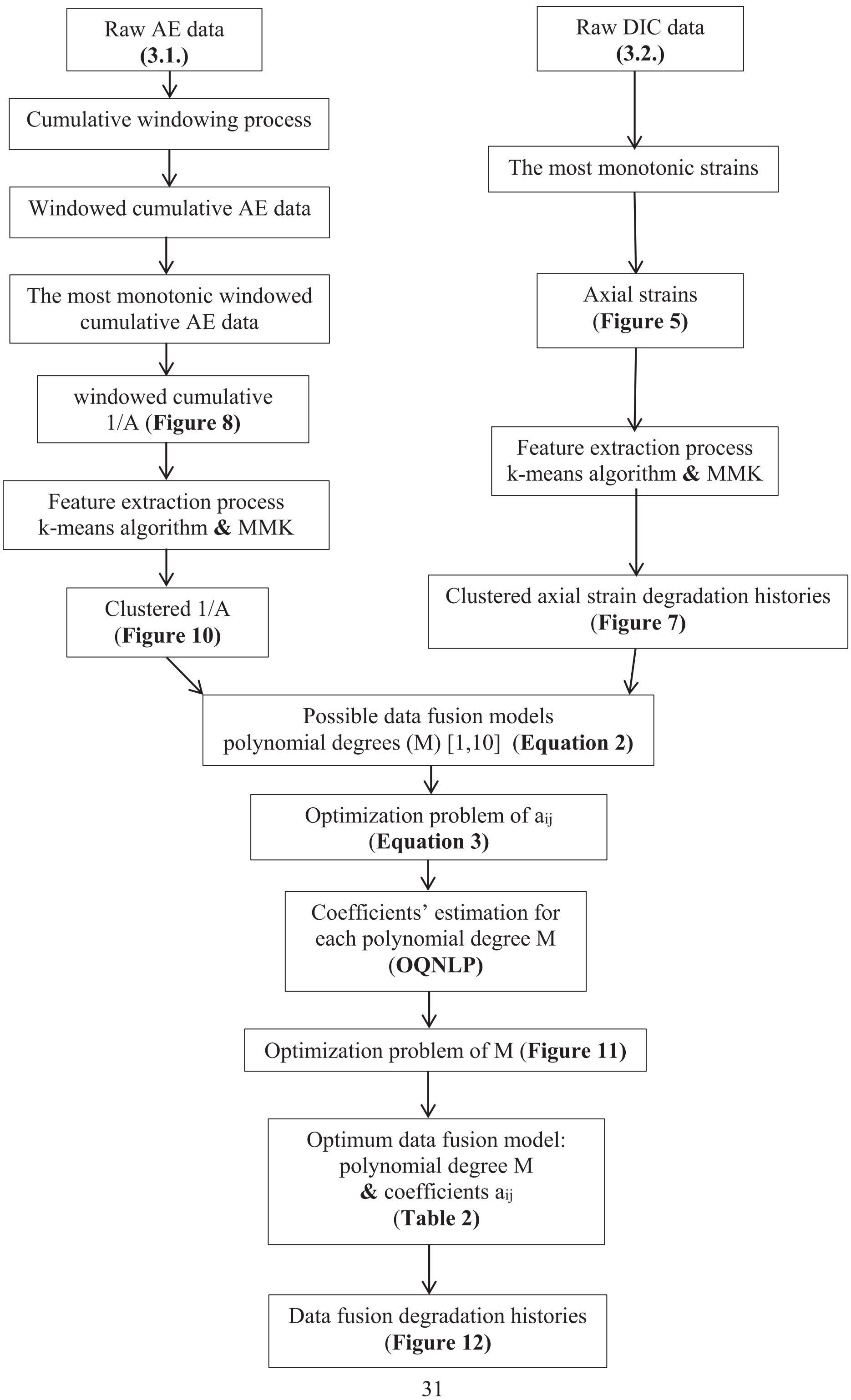
Raw AE data
(3.1.)
Cumulative windowing process
Windowed cumulative AE data
The most monotonic windowed cumulative AE data
windowed cumulative 1/A (Figure 8)
Feature extraction process k-means algorithm & MMK
Clustered 1/A (Figure 10)
Raw DIC data
(3.2.)
The most monotonic strains
Axial strains (Figure 5)
Feature extraction process k-means algorithm & MMK
Clustered axial strain degradation histories (Figure 7)
Possible data fusion models polynomial degrees (M) [1,10] (Equation 2)
Optimization problem of aij (Equation 3)
Coefficients' estimation for each polynomial degree M (OQNLP)
Optimization problem of M (Figure 11)
Optimum data fusion model: polynomial degree M & coefficients aij (Table 2)
Data fusion degradation histories (Figure 12)
31

References

[1] Williams JH, Davies A, Drake IR. Condition-based maintenance and machine diagnostics. Chapman and Hall; 1994. p. 187.
[2] Marseguerra M, Zio E, Podofillini L. Condition-based maintenance optimization by means of genetic algorithms and Monte Carlo simulation. Reliab Eng Syst Safety 2002:77151–65.
[3] Elattar HM, Elminir HK, Riad AM. Prognostics: a literature review. Complex Intell Syst 2016;2:125–54.
[4] Farrar CR, Lieven NAJ. Damage prognosis: the future of structural health monitoring. Phil Trans R Soc A 2007;365:623–32.
[5] Si XS, Wang W, Hu CH, Zhou DH. Remaining useful life estimation – A review on the statistical data driven approaches. Eur J Oper Res 2011;213:1–14.
[6] Chiachío J, Chiachío M, Saxena A, Sankararaman S, Rus G, Goebel K. Bayesian model selection and parameter estimation for fatigue damage progression models in composites. Int J Fatigue 2014;70:361–73.
[7] Chiachío J, Chiachío M, Sankararaman S, Saxena A, Goebel K. Condition-based prediction of time-dependent reliability in composites. Reliab Eng Syst Saf 2014;142:134–47.
[8] Corbetta M, Sbarufatti C, Giglio M, Saxena A, Goebel K. A Bayesian framework for fatigue life prediction of composite laminates under co-existing matrix cracks and delamination. Comp Struct 2018;187:58–70.
[9] Pascoe JA, Alderliesten RC, Benedictus R. Methods for the prediction of fatigue delamination growth in composites and adhesive bonds – a critical review. J Eng Fract Mech 2013;112-113:72–96.
[10] Carpinteri A, Paggi M. A unified interpretation of the power laws in fatigue and the analytical correlations between cyclic properties of engineering materials. Int J Fatigue 2009;31:1524–31.
[11] Liu Y, Mohanty S, Chattopadhyay A. A Gaussian Process based prognostics framework for composite structures. Proceedings of SPIE: modeling, signal processing, and control for smart structures, San Diego, March. 2009.
[12] Liu Y, Mohanty S, Chattopadhyay A. Condition based structural health monitoring and prognosis of composite structures under uniaxial and biaxial loading. J Nondestr Eval 2010;29:181–8.
[13] Eleftheroglou N, Loutas TH. Fatigue damage diagnostics and prognostics of composites utilizing structural health monitoring data and stochastic processes. Struct Health Monit 2016;15(4):473–88.
[14] Eleftheroglou N, Zarouchas D, Loutas TH, Alderliesten R, Benedictus R. Online remaining fatigue life prognosis for composite materials based on strain data and stochastic modeling. Key Eng Mater 2016;713(1662–9795):34–7.
[15] Loutas TH, Eleftheroglou N, Zarouchas D. A data-driven probabilistic framework towards the in-situ prognostics of fatigue life of composites based on acoustic emission data. Comp Struct 2017;161:522–9.
[16] Jefferson C, Vanniamparambil PA, Hazeli K, Bartoli I, Kontsos A. Damage quantification in polymer composites using a hybrid NDT approach. Compos Sci Technol 2013;83:11–21.
[17] Liu Z, Forsyth DS, Komorowski JP, Hanasaki K, Kirubarajan T. Survey: state of the art in NDE data fusion techniques. IEEE T-IM 2007;56(6):2435–51.
[18] Jiang S-F, Zhang C-M, Zhang S. Two-stage structural damage detection using fuzzy neural networks and data fusion techniques. Expert Syst Appl 2011;38(1):511–9.
[19] Gros XE. Multisensor data fusion and integration in NDT. Applications of NDT data fusion. US: Springer; 2001. p. 1–12.
[20] Hall DL, McMullen SAH. Mathematical techniques in multi-sensor data fusion. Boston: Artech House; 2004.
[21] Hall DL, Llinas J. An introduction to multisensor data fusion. Proc IEEE 1997;85(1):6–23.
[22] Zhao X, Li M, Song G, Xu J. Hierarchical ensemble-based data fusion for structural health monitoring. Smart Mater Struct 2010;19:4–045009.
[23] Zio E, Maio F. Failure prognostics by a data-driven similarity-based approach. Int J Rel, Qual Saf Eng 2013;20:135001.
[24] Coble J, Wesley HJ. Identifying optimal prognostic parameters from data: a genetic algorithms approach. Annual conference of the prognostics and health management society. September 2009.
[25] Qian F, Niu G. Remaining useful life prediction using ranking mutual information based monotonic health indicator. Prognostics and system health management conference. 2015.
[26] Liao L. Discovering prognostic features using genetic programming in remaining useful life prediction. IEEE Trans Ind Electron 2014;61(5):2464–72.
[27] McCarter D, Shumaker B, McConkey B, Hashemian H. Nuclear power plant instrumentation and control cable prognostics using indenter modulus measurements. Int J Progn Health Manage 2014;16(5):1–10.
[28] Yaguo L. Intelligent fault diagnosis and remaining useful life prediction of rotating machinery. Butterworth-Heinemann; 2016.
[29] Moghaddass R, Zuo MJ. An integrated framework for online diagnostic and prognostic health monitoring using a multistate deterioration process. Reliab Eng Syst Saf 2014;124:92–104.
[30] Moghaddass R, Zuo MJ. Multistate degradation and supervised estimation methods for a condition-monitored device. IIE Trans 2014;46(2):131–48.
[31] Jegou H, Douze M, Schmid C. Product quantization for nearest neighbor search. IEEE Trans Patten Anal Mach Intell 2011;33(1):117–28.
[32] Yue S, Pilon P. A comparison of the power of the t test, Mann–Kendall and bootstrap tests for trend detection. Hydrol Sci J 2004;49(1):21–38.
[33] Ugray Z, Lasdon L, Plummer J, Glover F, Kelley J, Marti R. Scatter search and local NLP solvers: a multistart framework for global optimization. INFORMS J Comp 2007;19(3):328–40.
[34] Saxena A, Celaya J, Saha B, Saha S, Goebel K. Metrics for offline evaluation of prognostic performance. Int J Progn Health Manage 2010;1:1–20.
[35] Peng T, He J, Xiang Y, Liu Y, Saxena A, Celaya J, Goedel K. Probabilistic fatigue damage prognosis of lap joint using Bayesian updating. J Intell Mater Syst Struct 2014. 1045389X14538328.
[36] Goebel K, Saha B, Saxena A. A comparison of three data-driven techniques for prognostics. 62nd meeting of the society for machinery failure prevention technology. 2008.
[37] Eleftheroglou N, Zarouchas D, Loutas TH. In-situ fatigue damage assessment of carbon-fibre reinforced polymer structures using advanced experimental technique. 17th European conference on composite materials. 2016.
[38] Lekhnitskii S.G., Tsai S.W., Cheron T.. Anisotropic plates. Gordon and Breach Science Publishers New York. New York; 1963.
[39] Tuegel E.J., Bell R.P., Berens A.P., Brussat T., Cardinal J.W., Gallagher J.P., Rudd J.. Aircraft structural reliability and risk analysis handbook. In: vol. 1, Basic analysis methods. No. AFRL-RQ-WP-TR-2013-0132. AIR FORCE RESEARCH LAB WRIGHT-PATTERSON AFB OH AEROSPACE SYSTEMS DIR; 2013.